

Atomistic simulation of frictional anisotropy on quasicrystal approximant surfaces

Zhijiang Ye and Ashlie Martini

*Department of Mechanical Engineering, University of California Merced,
5200 N. Lake Road, Merced, CA 95343, USA*

Patricia Thiel

*Departments of Chemistry and Materials Science and Engineering,
Iowa State University and the Ames Laboratory, Ames, IA*

Heather H. Lovelady, Keith McLaughlin, and David A. Rabson*

*Department of Physics, University of South Florida,
4202 E. Fowler Ave., Tampa, FL 33617, USA*

(Dated: October 3, 2018)

Abstract

Park *et al.* have reported eight times greater atomic-scale friction in the periodic than in the quasiperiodic direction on the two-fold face of a decagonal Al-Ni-Co quasicrystal [Science **309**, 1354 (2005)]. We present results of molecular-dynamics simulations intended to elucidate mechanisms behind this giant frictional anisotropy. Simulations of a bare atomic-force-microscope tip on several model substrates and under a variety of conditions failed to reproduce experimental results. On the other hand, including the experimental passivation of the tip with chains of hexadecane thiol, we reproduce qualitatively the experimental anisotropy in friction, finding evidence for entrainment of the organic chains in surface furrows parallel to the periodic direction.

Published: Phys. Rev. B **93**, 235438 (2016)

PACS numbers: 62.20.Qp, 61.44.Br, 68.35.Af, 68.37.Ps, 02.70.Ns

I. INTRODUCTION

The peculiarly low friction between quasicrystal surfaces and a contacting probe remains a puzzle.¹ Most of the proposed and realized applications of quasicrystals have taken advantage of this low friction.²⁻⁶ Anomalously low friction has been reported at length scales ranging from atomic probes to engineering pin-on-disk experiments, in air and in vacuum, and at such low normal forces as to avoid any surface damage, even at the atomic scale, as well as in ploughing experiments.⁷ Quasicrystals exhibit lower friction than related periodic phases, called approximants, of similar chemical composition,^{7,8} suggesting but not proving that more than surface chemistry is involved. At the same time, the lack of periodicity in quasicrystals makes them hard, and low friction could be a consequence of hardness.^{5,7,9-11} A 2005 experiment by Park *et al.* sought to dispense with all such surface-dependent effects by measuring the friction between a thiol-passivated atomic force microscope (AFM) probe and a two-fold surface of a decagonal AlNiCo quasicrystal.¹² On this surface, one direction is periodic, the other quasiperiodic. That surface damage was averted through the intervening thiol was demonstrated by STM imaging before and after the friction measurements. The experiment, in ultra-high vacuum, found an eight-fold anisotropy in the magnitude of sliding friction.

Such a large surface-friction anisotropy was virtually unknown in atomic-scale measurements; a recent review of theories of quasicrystal friction dubbed it the “giant frictional-anisotropy effect.”¹ Filippov *et al.*, attacking the problem computationally, reported reproducing the experimental anisotropy in a Langevin model in which mean feature spacings differed in the periodic and quasiperiodic directions; the quasiperiodicity itself was not relevant.¹³⁻¹⁵ However, three of us, using the same methods, found that small changes in the parameters could change the sense of the anisotropy and argued, moreover, that Filippov’s parameters did not correspond to scanning-tunneling-microscope (STM) images of the experimental surface.¹⁶

Other plausible explanations include entrainment of the thiol chains passivating the AFM tip and the difficulty of either exciting or propagating phonon or electronic modes. In such a complex system, it would not be surprising if each of these mechanisms played a role; on the other hand, the generic result of low friction in different quasicrystalline materials under different circumstances suggests a generic mechanism tied to quasicrystallinity.

Controversy over the frictional anisotropy on d-AlNiCo echoes controversy over the various contributions to atomic-scale friction on other surfaces that do not combine periodic and quasiperiodic order.¹⁷⁻²⁰ By testing each of the proposed mechanisms (except electronic), molecular-dynamics (MD) simulation on d-AlNiCo may provide clues to the nature of atomic-scale friction generally,²¹ and that is the purpose of the current paper.

We report MD friction simulations on two quasicrystal approximants as well as on a series of artificial “Fibonacci” samples approaching true quasiperiodicity. We searched for, but did not find, evidence for the phonon hypothesis. We find instead that simulation of the thiol molecules passivating the tip is necessary to produce substantial frictional anisotropy, and by examining surface topography, thiol configurations, and adhesion forces, argue that entrainment in furrows is responsible for at least some of the observed anisotropy.

II. METHODS

Perhaps the only simple aspect of the surfaces of quasicrystals is that they appear to reflect the underlying bulk structures without reconstruction.²² While these materials exhibit a high degree of long-range positional order, as demonstrated in Fourier space by very sharp diffraction peaks,²³ they do so without periodicity; in one sense, their unit cells are infinite. As a consequence, only a few bulk structures have been proposed at a level permitting comparison to experiment.²⁴ This poses a particular challenge to the simulation of atomic-scale friction on quasicrystal surfaces. However, quasicrystalline approximants contain local symmetries and structural motifs similar to those of their quasicrystalline counterparts²⁵ and are more suitable for MD simulations because of their periodicity.

In this work, we used two d-AlNiCo approximants supplied by Widom, H1 with a unit cell of 25 atoms and T11 with 343 atoms per unit cell.²⁶ These crystal structures were repeated in space to create model substrates. The apex of an AFM tip was then introduced into the models to enable simulations of sliding friction. The size and sliding surface of the approximant sample and the size, shape, and material of the tip were varied. The tip was subjected to a normal load and slid across the substrate surface in two orthogonal directions, corresponding to periodicity and (approximate) quasiperiodicity on the sample surface. Friction was then calculated as the time average of the lateral force resisting that sliding. In all cases, temperature was controlled using a Langevin thermostat, and the

simulations were run using the LAMMPS simulation software.²⁷ In what follows, references to the “quasiperiodic” direction are intended in the sense of an approximant, thus referring to the larger of the two periodicities.

III. ADAMANT TIP ON D-ALNICO APPROXIMANTS

The first model we discuss consisted of 1,250 unit cells of the 25-atom H1 approximant (31,250 atoms) and an “adamant” slab tip (3,250 atoms) moving laterally across its surface (Fig. 1a).²⁸ Interactions among the Al, Ni, and Co atoms of the approximant were described by a set of pair potentials designed for this system by Widom and Moriarty,^{29–31} truncated at 0.7 nm. The adamant of the tip was a fictitious atom of the same mass as aluminum forming a very hard and inert FCC solid. Adamant-adamant pair interactions were given by the Widom-Moriarty Al-Al potential multiplied by 10, while the purely repulsive force with any atom in the approximant was $b \exp(-r/a)$, r the pair separation, $b = 100$ eV, and $a = 1$ Å. The top-most layers of the tip were treated as a rigid body and the bottom-most layers of the approximant fixed. The center layers of the tip and approximant were subject to the thermostat in the direction perpendicular to sliding to control the temperature of the simulation at less than 1K.³² The remaining atoms in the system were free to evolve according to NVE dynamics (constant number, constant volume, and constant energy). A normal force was applied by moving the tip downward towards the substrate after which the tip was slid across the substrate at 5 m/s.

Fig. 1 shows results for loads between 7.3 nN and 95.7 nN and sliding speeds between 4 and 12 m/s. For each speed and at lower loads, the frictional force in the quasiperiodic direction was slightly higher than in the periodic direction. This trend is opposite that expected based on the experiment. Using the higher loads, the ratios of lateral to normal force in Fig. 1, *i.e.*, coefficient of friction, could be fit linearly, and there was a small anisotropy in the expected direction with the periodic coefficient of friction higher than quasiperiodic by about 11%. However, both frictional force and frictional coefficient were orders of magnitude smaller than those reported experimentally.

To improve the physical realism of the simulation, we replaced the H1 approximant with the larger-unit-cell T11 approximant. The larger approximant unit cell contains more different local environments, reproduces larger structural motifs from the quasicrystal, and

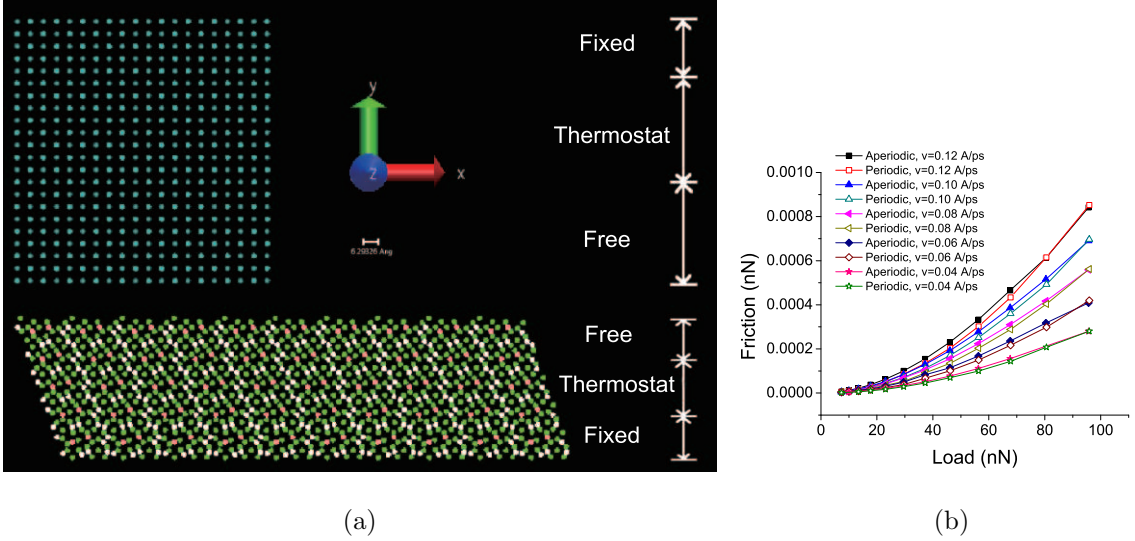


FIG. 1: (a) Snapshot of a run on the H1 approximant showing adamant tip upper-left and facing the 10-fold surface of the approximant. The x direction is the (approximately) quasiperiodic direction for the 2-fold surface, z the periodic direction. Green spheres are Al, white Ni, pink Co, and blue adamant. (b) Average friction force increasing with load from a simulation of an adamant slab sliding on an H1 approximant. Anisotropy is small and, in most cases, the trend is opposite the experimentally observed anisotropy; the magnitudes of the friction force and friction coefficient are also much smaller than expected.

should more closely approximate the experimental sample. Runs were performed on a sample of 8 unit cells (2,744 atoms). The cuboid-shaped tip was constructed of 340 FCC aluminum atoms but treated as a rigid body. In this case, to capture the compliance of an AFM system, we connected the tip to a virtual atom using a harmonic spring (spring constant 16 N/m) and moved the virtual atom across the substrate. The sliding speed was 5 m/s and the target temperature 0K. Figure 2 compares two different approximant surface terminations to the atomic surface model derived from STM images in Ref. [33]. On relaxation, both terminations yield Al-rich surfaces compatible with the model; notable features include pentagons with a single vertex exposed to the surface, distorted pentagons with two vertices on the surface, and short and long motifs with lengths in the ratio of the Golden Mean, as in the Fibonacci sequence. The friction results are shown in Fig. 3. Again, neither termination exhibits the experimental anisotropy with larger friction in the periodic direction. Other runs, with sliding speeds as low 0.01 m/s, larger simulations (50,993 atoms), different spring

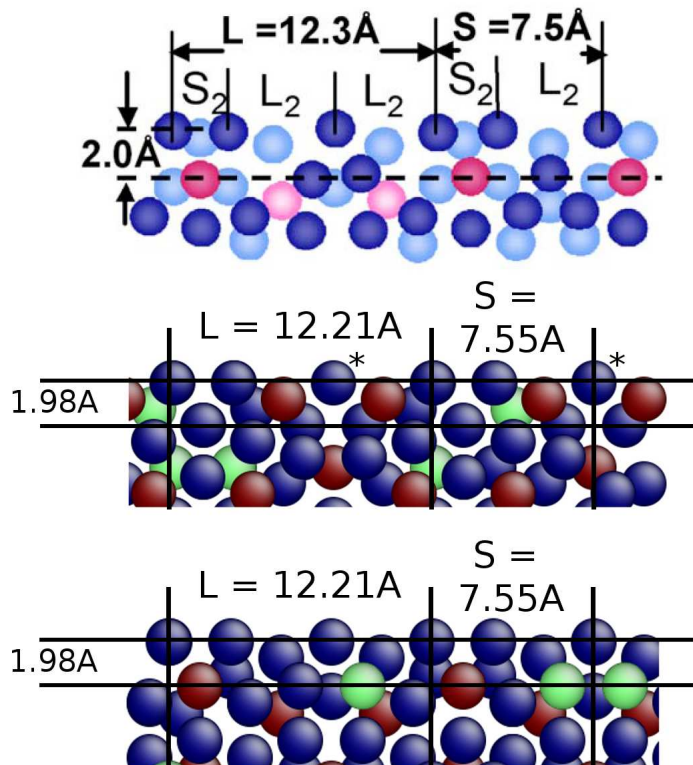


FIG. 2: (Top) Experimental surface model from [33]. The blue atoms are aluminum, pink transition metals. The T11 surface terminations in the middle and bottom panels both show features in common with the experimental model. Here, blue atoms are aluminum, red cobalt, and green nickel. Atoms marked (*) in the middle panel were unstable and so removed before friction simulation.

constants (16 or 8 N/m), and temperatures (0K or 300K) also failed to reproduce the experimental anisotropy.³⁴

IV. FIBONACCIUM AS A GENERICALLY QUASIPERIODIC SUBSTRATE

Only a few realistic approximant structures are available along with pair potentials that stabilize them, making it difficult to increase unit-cell size systematically in the approach to quasiperiodicity. One way around this difficulty is to simulate an entirely artificial substrate for which approximants are easily generated. The Fibonacci sequence has been used in various studies as a model of quasiperiodicity^{35–38} and in some cases has been expanded to the two-dimensional case.^{39,40} Adopting this geometry, we construct a “Fibonacci” solid

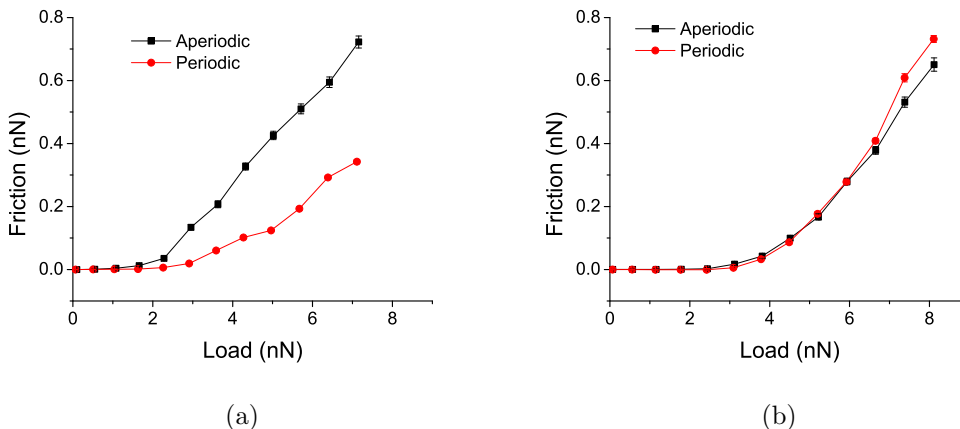


FIG. 3: Average friction force increasing with load from a simulation of a rigid FCC aluminum block sliding on terminations T11(a) and T11(b) of Figure 2. Although the magnitude of the friction is realistic, the frictional anisotropy seen in experiments is not reproduced.

in which the atoms occupy the sites of a simple-cubic lattice but vary in mass according to the Fibonacci sequence (...LSLLS...) in two dimensions, resulting in a large mass (m_{LL}) on grid sites for which both coordinates are L , a small mass (m_{SS}) where both coordinates are S , and an intermediate mass ($m_{LS} = m_{SL} = [m_{LL} + m_{SS}]/2$) on grid sites with L in one coordinate and S in the other. These two-dimensional grids stack periodically in the third direction. The artificial structure is stabilized with a simple pair potential. Details of the approach are available elsewhere.³⁴ We varied the order of the Fibonacci approximant, temperature, sliding speed, and spring constant, but no combination of these parameters yielded the experimentally-observed anisotropic friction. Representative results from simulations for samples generated using period-3 and period-55 Fibonacci sequences are shown in Fig. 4. If this were a real layered material, the linear period of 55, corresponding to a two-dimensional unit cell of 3,025, would be quite large and so substitutes for exact quasiperiodicity. However, the experimental anisotropy is not present.

V. BARE AL TIP ON H1 APPROXIMANT

Seeing no anisotropy in the generic Fibonacci model, we pursued instead more realistic simulations of the experimental system. New parameters to describe Al-Ni-Co alloys,⁴¹ compounds, and mixtures using the Embedded Atom Method (EAM)⁴² were recently made

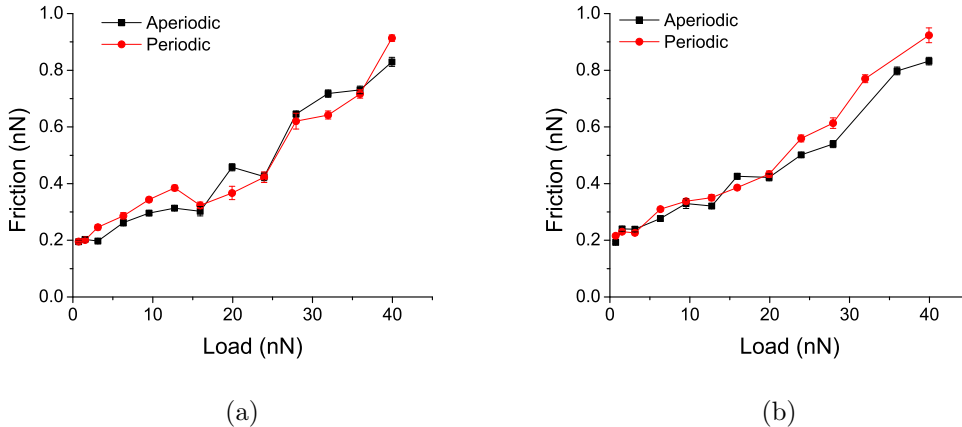


FIG. 4: Average friction force increasing with load from a simulation of sliding on a substrate generated based on (a) period-3 and (b) period-55 Fibonacci sequences. The frictional anisotropy of the experiments is not captured by the simulation.

available via the NIST Interatomic Potentials Repository Project⁴³ based on the binary Ni-Al potential⁴⁴ and elemental Co potential.⁴⁵ We used this model to describe the interactions within the previously described H1-approximant sample. The Al model tip was also modified by cutting atoms from the original slab into a 2 nm radius hemisphere. The uppermost atoms of the tip were treated as a rigid body and pulled along the substrate at 5 m/s by a virtual atom connected via a harmonic spring with spring constant 16 N/m. This model is illustrated in Fig. 5 (upper). The bottom-most layers of atoms in the substrate were fixed. All unconstrained atoms in the system were coupled to a Langevin thermostat in the two directions orthogonal to sliding with a target temperature of 300K.

Fig. 6 shows the average friction of the hemispherical tip sliding on the H1-approximant substrate at different loads. We observed that, while the simulation captures frictional anisotropy, it is the opposite direction of that observed in experiments, *i.e.*, friction is smaller in the periodic direction. In addition, we observed significant substrate wear, even at moderate loads, and so could not run the simulation at loads larger than ~ 6 nN.

VI. THIOL-PASSIVATED TIP

The observation of wear from a bare tip is actually consistent with experimental observation and is also the reason that the experiments used a TiN tip passivated with hexadecane

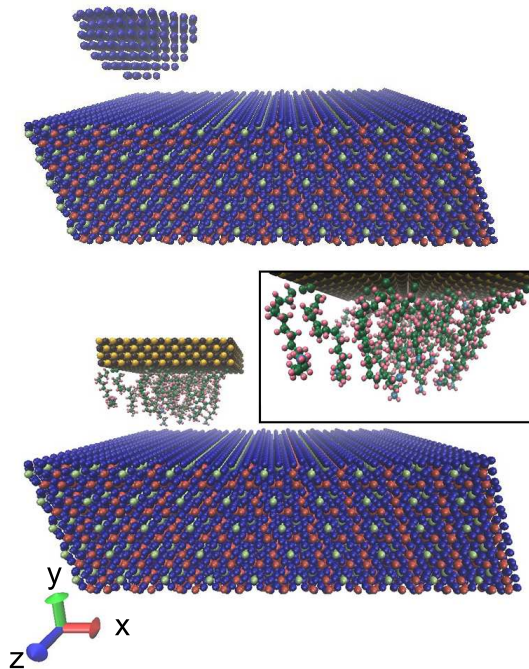


FIG. 5: MD models of a hemispherical tip (upper image) and a thiol-passivated TiN tip (lower image and inset) sliding on d-AlNiCo substrate. Spheres represent atom positions where colors correspond to different elements: yellow - Ti, black - N, dark green - C, light blue - S, pink - H, red - Co, green - Ni, blue - Al.

thiol,^{12,46,47} eliminating wear, as verified by STM imaging before and after. To capture this in the simulation, we constructed a new model of a thiol-passivated TiN tip to mimic that used in experiments. The model system is illustrated in Fig. 5(b). We first created models of a block of TiN ($40 \times 10 \times 40 \text{ \AA}$) and 20 thiol molecules using Accelrys Materials Studio. Then, we transferred the structures into LAMMPS and artificially increased the interaction strength between the bottom surface atoms of the TiN tip and the carbon atom at one end of each thiol molecule so that one end of the thiol molecules was attached to the TiN bottom surface after equilibration. The TiN slab was subsequently treated as a rigid body. The Polymer Consistent Force Field (PCFF) was used to describe bond, angle, torsion, and out-of-plane interactions between all tip (TiN and thiol) atoms, the EAM potential was again used to describe the inter-atomic interactions between substrate atoms, and the Lennard-Jones (LJ) potential was used to model the long-range interactions between tip and substrate with parameters obtained using Lorentz-Berthelot mixing rules. All other

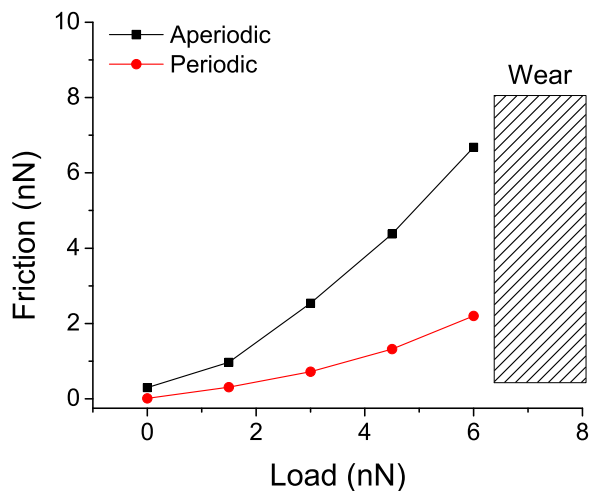


FIG. 6: Average friction force increasing with load for a hemispherical aluminum tip sliding on an H1 approximant substrate. Friction magnitude is reasonable, but the frictional anisotropy is opposite to that observed in previous experiments. Wear was observed at even moderate loads, precluding characterization of friction above ~ 6 nN.

simulation parameters and conditions were the same as described for the hemispherical Al tip model.

Fig. 7 shows the average friction of the thiol-passivated TiN tip sliding on the H1-approximant substrate at different loads. We observed higher friction in the periodic direction than the quasiperiodic direction, consistent with the trend observed in experiments. The magnitude of the friction and friction coefficient were also roughly comparable to the experiments, although the anisotropy was much smaller. In this case, we did not observe any noticeable wear on the surface, confirming that the thiol molecules indeed contributed to reducing wear.

Since frictional measurements are noisy, verifying the anisotropy in Figure 7 requires an analysis of the uncertainties. Figure 8 shows a sample run at 80 nN load in the quasiperiodic direction: the noise is large compared to the time-averaged friction. A pseudo-period of ~ 98 ps, possibly reminiscent of stick-slip friction, is evident in the time series; a similar pseudo-periodicity was observed in the periodic direction. Although experimentally stick-slip has been reported absent or suppressed at low loads in true quasicrystals,^{8,46,48} we would still expect it in this low-order approximant. A power-spectral estimate shows a broad peak

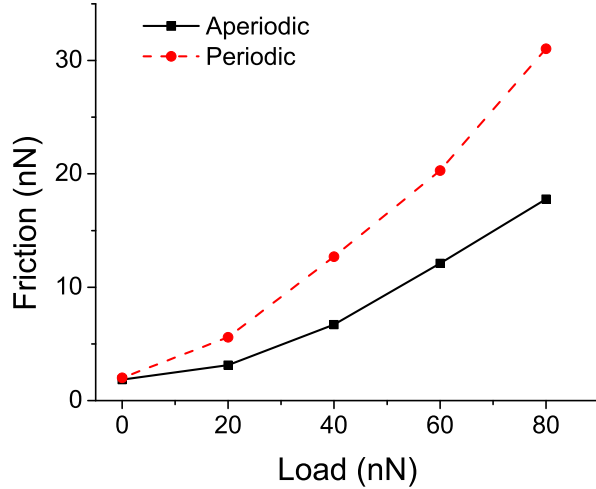


FIG. 7: Average friction force increasing with load for a thiol-passivated TiN tip sliding on the H1 approximant substrate. No surface wear is observed, and both the magnitude and the anisotropy of the friction are roughly consistent with experiment.

closer to 82 ps than 98 ps, and we shall use this periodicity in estimating error bars. At the sliding speed of 5 m/s, this periodicity also corresponds closely to the approximant unit-cell size of 4.03 Å, although in other runs, there were differences between the stick-slip-like pseudo-periodicity and corresponding unit-cell dimension as large as 20%.

Fig. 8 suggests initial transient behavior that subsides by 300 ps. In these runs, we averaged only data past 400 ps. Table I presents the mean friction values with error bars. To estimate error bars, we collected the data past 400 ps into N bins each of duration equal to the pseudo-period so that the mean friction in each bin is considered an independent measurement. The error bars are then estimated as a sample standard deviation of the bins divided by \sqrt{N} . Since the pseudo-periods are themselves uncertain, we compared the means and estimated error bars for pseudo-periods 20% larger, 20% smaller, twice as large, and half as large as that extracted from the power spectrum. The table displays as “worst” the estimate with the largest error bar. In each case, the results show a highly significant anisotropy of order 60%–75% with negligible sensitivity to the binning procedure.

One hypothesis for the origin of the frictional anisotropy has involved the difficulty of exciting or propagating phonons through the quasicrystal in the quasiperiodic direction. We

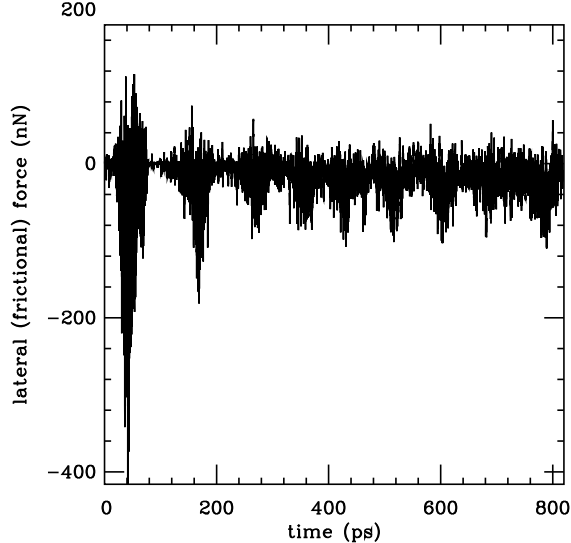


FIG. 8: Sample run from Figure 7 for the quasiperiodic direction at 80 nN load. The time series is noisy, but the pseudoperiod of $\sim 82\text{--}98$ ps enables us to estimate error bars of smaller than 1.5 nN to the average negative lateral force of 18.7 nN. (The first 400 ps are excluded in computing the average.)

TABLE I: Frictional forces under 80 nN load with estimated uncertainties. Runs with rigid substrates eliminate lattice-vibration effects. For each type of substrate (non-rigid and rigid), the first row gives the frictional forces along the periodic and quasiperiodic directions. Friction and error bars in nN are estimated from equal-duration bins given by the pseudo-period, with the error bar the standard deviation of the mean of the independent bins. The row labeled “worst” for each substrate type substitutes the pseudo-period and error bar derived from an alternative binning procedure in which the bins are either as given previously, 20% larger or smaller, or twice or half as large, *whichever yields the largest error bar*. For both substrates, the periodic friction is larger than the quasiperiodic by at least seven standard deviations of the mean.

| substrate | periodic friction | quasiperiodic friction |
|--------------|-------------------|------------------------|
| non-rigid | 30.8(1.0) | 18.7(0.9) |
| <i>worst</i> | <i>30.8(1.7)</i> | <i>18.4(1.5)</i> |
| rigid | 39.2(1.5) | 22.1(1.2) |
| <i>worst</i> | <i>39.2(1.5)</i> | <i>22.1(2.1)</i> |

can test this by suppressing lattice vibrations entirely using simulations where the atoms in the substrate are artificially fixed in place after equilibration. If phonons were important, we might expect the anisotropy to decrease for the rigid substrate and for the overall friction to be lower. Table I shows exactly the opposite: the overall friction increases 20–30%, while the anisotropy remains approximately the same or increases slightly on the rigid substrate. With the substrate atoms fixed, the only degrees of freedom left are in the thiol-passivated tip. The difference in friction between the two cases could result from the depression of surface asperities in the non-rigid case, something we see when we plot atomic positions. On both substrates, however, the friction was higher in the periodic direction.

In order to understand why the thiol-passivated tip model was successfully able to capture the expected friction trends, we characterized the trajectory of the last carbon atom in the thiol chains as the tip slid. Figure 9 illustrates the vertical height distribution of the quasicrystal surface as gray-scale maps, where the lighter gray corresponds to a lower vertical position. We can identify parallel furrows (low vertical positions) and peaks (high vertical positions) in the gray map due to the periodic surface structure of the quasicrystal. The colored lines indicate the trajectories of the last carbon atom in six representative thiol chains. We observed very different trajectories during sliding in the periodic and quasiperiodic directions. Most significantly, for sliding in the periodic direction (z-direction) illustrated in Fig. 9(a), the trajectories remained, on average, in the light colored regions on the gray-scale surface-height map, indicating that the chains were entrained in the surface furrows. This entrainment could contribute to adhesive friction. In contrast, for sliding in the quasiperiodic direction (x-direction) illustrated in Fig. 9(b), the thiol chain tail trajectories exhibited irregular motion patterns corresponding to limited chain entrainment.

Fig. 10 provides additional evidence for entrainment of thiol chains in furrows when the tip is dragged in the periodic direction. This shows a kernel-smoothed distribution (kernel width 0.3 \AA) of lateral carbon positions for all carbon atoms at heights less than about 2.6 \AA above the highest nominal (undepressed) surface-atom center, excluding the first 400 ps of the simulation. Split peaks centered at 6.3 \AA , 19.9 \AA , and 31.6 \AA are roughly consistent with the known furrow centers at lateral positions $(6.61 + 12.22n) \text{ \AA}$ for integer n , where 12.22 \AA is the approximant periodicity. Figures 9 and 10b show relatively shallow furrows with centers near these positions. A column of Al atoms divides each furrow in two. The splitting of the peaks could be due to this column or indicate affinity of carbons for the

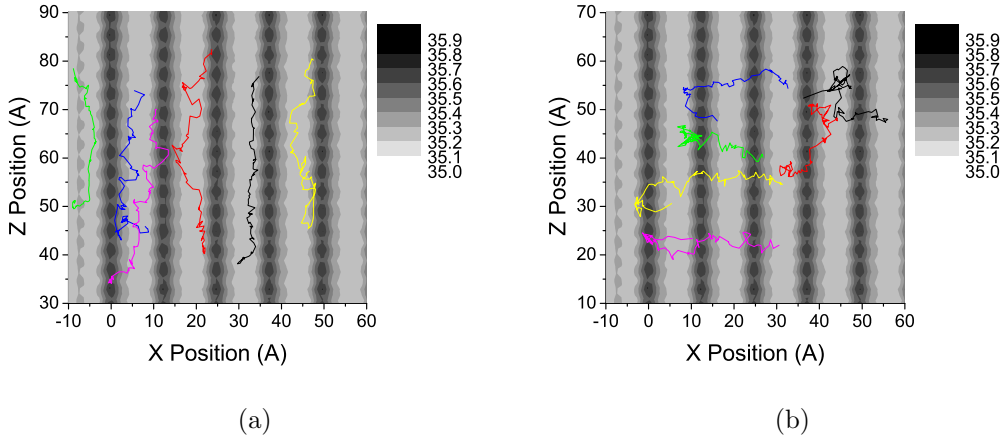


FIG. 9: The trajectories of the last carbon atom in the thiol chains when the tip slid in the (a) z -direction (periodic) and (b) x -direction (quasiperiodic). The z -periodicity is 4.03\AA , while the periodicity of the approximant in the quasiperiodic x direction is 12.22\AA . The gray-scale maps show the vertical heights of the quasicrystal surface in Angstroms.

furrow sides. We count carbon atoms at heights less than or equal to the nominal surface height as “in” the furrows and find 3.6 times as many such carbons when the tip is dragged in the periodic direction as when dragged in the quasiperiodic direction.

Figure 11 shows adhesive energies and maximum forces for runs at 80 nN load stopped at times between 100 ps and 800 ps. After the sliding is stopped, the tip is separated from the substrate, up to a height of 3.2 nm (somewhat longer than the length of a thiol chain, 2.4 nm). We calculated the force on the tip as a function of distance from the substrate during lift-off. The left half of the figure shows total integrated adhesive energy, the right half, the maximum force. Both show substantially greater adhesion after runs in the periodic direction. Both also level off by 400 ps, supporting our previously cited evidence that a steady state is reached by that time. Since the aluminum tip starts off at the same height above the surface in all cases, the differences in measures of adhesion must pertain to the thiol chains. We note that after short runs, there is essentially no difference in lift-off force or integrated adhesive energy, but after the chains have stretched out along the surface and, as we have argued, find themselves entrained in the furrows, the anisotropy becomes clear. Entrainment of thiols in furrows and the consequent higher adhesive force when the tip is dragged in the periodic direction could contribute to increased friction.

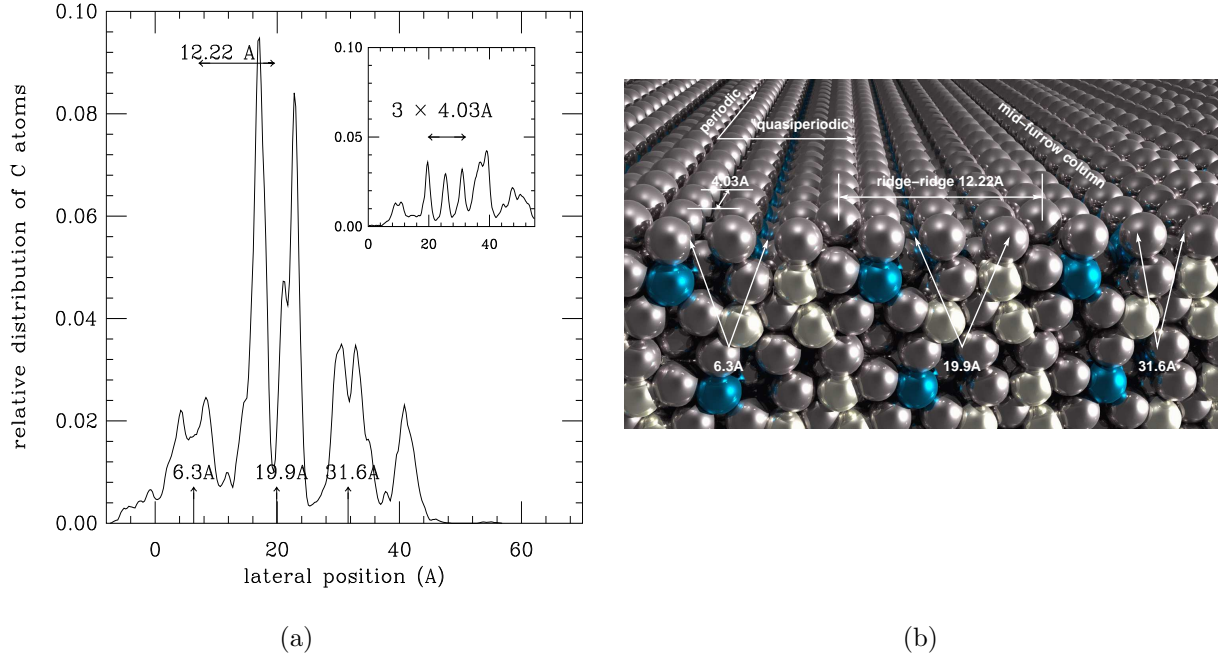


FIG. 10: (a) Relative distribution of lateral position of carbon atoms during the second half of the simulation dragging in the periodic direction (*i.e.*, the position axis is along the *quasiperiodic* direction.) Only atoms with absolute height less than 38 \AA , about 2.6 \AA above the nominal surface height, are counted. Split peaks centered at 6.3 \AA , 19.9 \AA , and 31.6 \AA are consistent with carbons localized near furrow edges, where the furrows are spaced 12.22 \AA apart. The smoothing kernel has a standard deviation of 0.3 \AA . Inset: distribution of lateral position for an aperiodic run (so the position axis runs along the periodic direction). Several pairs of adjacent peaks are spaced approximately 5.7 \AA apart, not corresponding to any surface features or to the 4.03 \AA periodicity. (b) Quasicrystal approximant surface, showing approximant periodicities of 12.22 \AA and 4.03 \AA and furrows aligned along the periodic direction (into the picture, periodicity 4.03 \AA). Each furrow is divided in two by a column of Al atoms, while the walls of the furrows consist of a higher “ridge” of three more tightly packed Al columns. Arrows mark the split peaks in Fig. 10a, labeled by the position half-way between the two parts and corresponding to the centers of shallow furrows as illustrated here and in the height maps of Fig. 9. Note five-fold motifs on the ten-fold surface, facing forward.

VII. DISCUSSION

Explaining the giant frictional anisotropy observed on the two-fold surface of d-AlNiCo requires attention to realistic details; generic models showed no anisotropy, or showed reversed anisotropy, or proved sensitive to parameters. Comparison of the two terminations of the T11 approximant, in which the less stable termination appeared to show a substantial

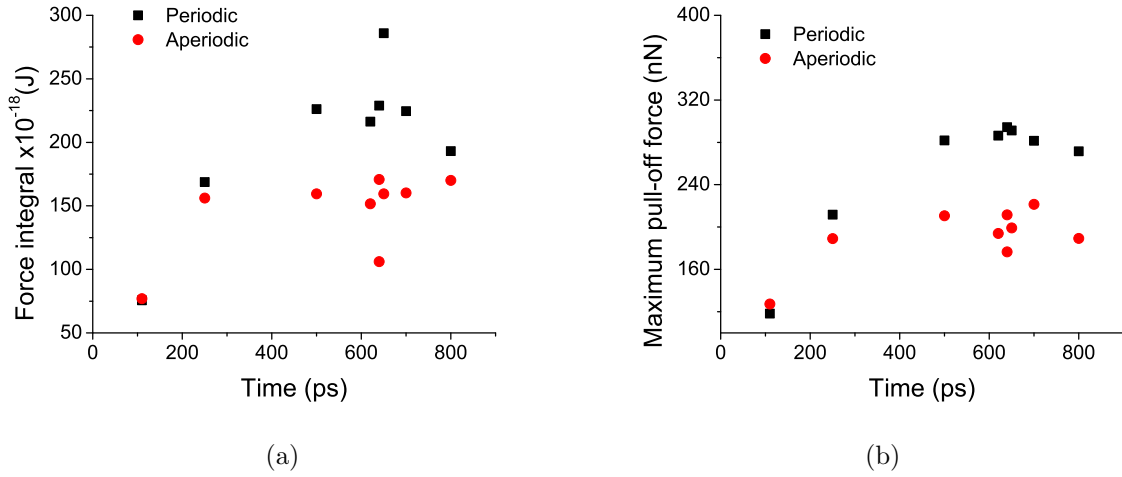


FIG. 11: Adhesive energies (left) and maximum adhesive forces during lift-off (right) after runs at 80 nN load of durations between 100 ps and 800 ps. Since the aluminum tip is starting from the same height in all cases, any differences must pertain to the thiol chains. The graphs show greater adhesion for runs in the periodic direction, consistent with entrainment of the chains in furrows.

reversed frictional anisotropy (quasiperiodic direction with higher friction) demonstrates an unanticipated dependence on details of surface structure.

Moreover, in order to avoid surface damage, it is necessary to minimize adhesive forces, either artificially through the use of purely repulsive pair potentials (as in “adamant”) or directly by simulating the thiol passivation. We have seen that the former results in unrealistically small frictional forces and may miss important physics.

Entrainment of organic chains in surface furrows provides an intuitively attractive mechanism for anisotropy on this surface. When the tip moves in the periodic direction, parallel to the furrows, the chains preferentially stay aligned, and their adhesion to the furrow sides may contribute to friction. Conversely, when the tip moves perpendicularly, the chains splay in apparently random configurations; additionally, these configurations may change frequently as the chains move across successive ridges in the (approximately) quasiperiodic direction, minimizing adhesion. Of course, this mechanism does not actually depend on quasiperiodicity; the H1 unit cell realizes only the 1/1 approximant to the golden mean. The idea that local topographic features, rather than quasiperiodicity, could control the anisotropy has also been advanced by Filippov *et al.*^{13–15} Using a Langevin model over an

external potential representing the substrate, rather than molecular dynamics, the authors suggest that larger force gradients on the atomic scale in the periodic direction could explain the anisotropy. However, the parameters in that model have been questioned,¹⁶ and small changes can lead to a reversed anisotropy. The furrow model on the other hand, makes no *ad-hoc* assumptions about effective atomic shapes and should be robust against uncertainties in structural determination.

We note a possible connection between approximant quasiperiodicity and the existence of surface furrows that will survive the limit of perfect quasiperiodicity. Spacings between rows, as in the surface Al atoms in Fig. 10b, follow the Fibonacci sequence (...LSLLS...), as suggested even in the approximant of the figure. If the short (“S”) spacings tend to squeeze rows and push them up relative to the long, we could arrive generically at the sort of surface corrugation invoked here.

The furrow model does not come close to the eight-fold observed anisotropy in frictional force. Sliding velocities in these simulations were much larger than in the experiment, and it is possible that one would see larger effects at realistic speeds, if they could be achieved.

However, any model relying solely on local topographic features fails to answer the question of why surface friction appears to be lower on the doubly quasiperiodic surfaces of true quasicrystals than on approximants, and lower on the approximants than on other phases in these alloy systems. Nor does it address why quasicrystals show lower friction in engineering-scale pin-on-disk experiments in air, with ploughing through an oxide layer, as well as in nanoscale experiments in vacuum.⁷

The Fibonacci model was designed to test the idea that the difficulty of either exciting or propagating phonons in a quasiperiodic direction of a quasicrystal having both periodic and quasiperiodic directions could account for the anisotropy. These runs found no such effect, and although theoretically phonon spectra in a quasicrystal should exhibit a dense set of gaps,^{35,49} experiments find mostly isotropic elastic properties.^{50,51} That friction, likewise, appears isotropic in a model capturing the quasiperiodicity of real quasicrystals while ignoring their topography, weakens the case for the phonon hypothesis.

There are at least three ways out. First, none of the simulations attempted to date considers electronic excitations, which may play a role.¹⁹ Second, unrealistic aspects of molecular dynamics, such as scan speeds or finite-size effects, may obscure physical mechanisms.

Finally, it may be that we’re looking at two different effects. The giant frictional

anisotropy on the two-fold surface of d-AlNiCo may in fact be due entirely to local topographic features, such as thiol-chain entrainment, having nothing to do with quasiperiodicity, while the relatively low friction of quasicrystal surfaces compared to those of approximants, and of approximants compared to other periodic phases, could be due to the greater hardness of the quasicrystals and to a pseudogap in the density of electronic states.^{1,52} Both are definite effects of quasiperiodicity for the quasicrystals and of unit-cell size for the approximants. Both are neatly factored out on the two-fold quasicrystal surface, possibly leaving topography as the only feature different in the two directions.

VIII. ACKNOWLEDGMENTS

We thank Susan Sinnott and Jacob Israelachvili for useful suggestions and Dr. Gustavo Brunetto for generating the ray-tracing image shown in Fig. 10b. Computations were performed on the CIRCE cluster at the University of South Florida and the Coates/Conte/Carter clusters at Purdue University. The initial atomic configuration of the thiol tip model was created with the assistance of U.S. Ramasamy. AM and ZY acknowledge the support of the National Science Foundation through grant CMMI-1362565. PT acknowledges support from the Office of Science, Basic Energy Sciences, Materials Sciences and Engineering Division of the U.S. Department of Energy (USDOE), under Contract No. DE-AC02-07CH11358 with the U.S. Department of Energy. DAR acknowledges NSF MRI award CHE 1531590 and the support of the Research-Computing group at the University of South Florida.

* davidra@ewald.cas.usf.edu

¹ D. A. Rabson, *Progress in Surface Science* **87**, 253 (2012).

² J.-M. Dubois and P. Weinland, “Matériaux de revêtement pour alliages métalliques et métaux,” Organisation Mondiale de la Propriété Intellectuelle brevet no. WO 90/01567 (1990), European patent registry number EP0356287 (1990); original French patent application number 8810559 from 1988.

³ J. M. Dubois, A. Proner, B. Bucaille, P. Cathonnet, C. Dong, V. Richard, A. Pianelli, Y. Massiani, S. Aityaazza, and E. Belinfeffe, *Annales de Chimie—Science des Matériaux* **19**, 3 (1994).

- ⁴ O. G. Symko, T. Klein, and D. Kieda, “Formation and applications of AlCuFe quasicrystalline thin films,” United-States Patent number 6,294,030 B1 (2001).
- ⁵ J.-M. Dubois, *Materials Science and Engineering: A* **294–296**, 4 (2000).
- ⁶ J. M. Dubois, *Israel Journal of chemistry* **51**, 1168 (2011).
- ⁷ J. Y. Park and P. A. Thiel, *J. Phys.: Cond. Mat.* **20**, 314012 (2008).
- ⁸ C. Mancinelli, C. J. Jenks, P. A. Thiel, and A. J. Gellman, *Journal of Materials Research* **18**, 1447 (2003).
- ⁹ K. Urban, M. Wollgarten, and R. Wittmann, *Physica Scripta* **T49**, 360 (1993).
- ¹⁰ K. Urban, M. Feuerbacher, M. Wollgarten, M. Bartsch, and U. Messerschmidt, in *Physical Properties of Quasicrystals*, edited by Z. M. Stadnik (Springer, Berlin, 1999) Chap. 11, pp. 361–401.
- ¹¹ P. Brunet, L.-M. Zhang, D. J. Sordelet, M. Besser, and J.-M. Dubois, *Mats. Sci. Engr.* **294–296**, 74 (2000).
- ¹² J. Y. Park, D. F. Ogletree, M. Salmeron, R. A. Ribeiro, P. C. Canfield, C. J. Jenks, and P. A. Thiel, *Science* **309**, 1354 (2005).
- ¹³ A. E. Filippov, A. Vanossi, and M. Urbakh, *Physical review letters* **104**, 074302 (2010).
- ¹⁴ A. E. Filippov, A. Vanossi, and M. Urbakh, *Phys. Rev. Lett.* **104**, 149901(E) (2010).
- ¹⁵ A. E. Filippov, A. Vanossi, and M. Urbakh, *Phys. Rev. Lett.* **107**, 209402 (2011).
- ¹⁶ K. McLaughlin, D. Rabson, and P. Thiel, *Phys. Rev. Lett.* **107**, 209401 (2011).
- ¹⁷ R. G. Tobin, *Phys. Rev. B* **48**, 15468 (1993).
- ¹⁸ J. B. Sokoloff, *Phys. Rev. B* **52**, 5318 (1995).
- ¹⁹ J. Krim, C. Daly, and A. Dayo, *Trib. Lett.* **1**, 211 (1995).
- ²⁰ A. Dayo, W. Alnasrallah, and J. Krim, *Phys. Rev. Lett.* **80**, 1690 (1998).
- ²¹ Y. Dong, Q. Li, and A. Martini, *Journal of Vacuum Science and Technology A* **31**, 030801 (2013).
- ²² R. McGrath, J. A. Smerdon, H. R. Sharma, W. Theis, and J. Ledieu, *J. Phys.: Cond. Mat.* **22**, 084022.1 (2010).
- ²³ S. W. Kycia, A. I. Goldman, T. A. Lograsso, D. W. Delaney, D. Black, M. Sutton, E. Dufresne, R. Brüning, and B. Rodricks, *Phys. Rev. B* **48**, 3544 (1993).
- ²⁴ H. Takakura, C. P. Gómez, A. Yamamoto, M. de Boissieu, and A.-P. Tsai, *Nature Materials* **6**, 58 (2007).

- ²⁵ C. L. Henley, *Physical Review B* **43**, 993 (1991).
- ²⁶ M. Widom, Private communication.
- ²⁷ S. Plimpton, *Journal of Computational Physics* **117**, 1 (1995).
- ²⁸ H. M. Harper, *A Molecular-Dynamics Study of the Frictional Anisotropy on the 2-fold Surface of a d-AlNiCo Quasicrystalline Approximant*, Master's thesis, University of South Florida (2008).
- ²⁹ J. A. Moriarty and M. Widom, *Physical Review B* **56**, 7905 (1997).
- ³⁰ M. Widom, I. Al-Lehyani, and J. A. Moriarty, *Physical Review B* **62**, 3648 (2000).
- ³¹ M. Widom and J. A. Moriarty, *Physical Review B* **58**, 8967 (1998).
- ³² An isotropic thermostat at an earlier stage of the investigation introduced significant noise; restricting the thermostat to the z direction^{53,54} reduced the noise. If the phonon hypothesis had been correct, the lateral thermostat could have masked the effect.
- ³³ J. Y. Park, D. F. Ogletree, M. Salmeron, R. A. Ribeiro, P. C. Canfield, C. J. Jenks, and P. A. Thiel, *Phys. Rev. B* **72**, 220201R (2005).
- ³⁴ K. McLaughlin, *Towards Understanding Low Surface Friction on Quasiperiodic Surfaces*, Master's thesis, University of South Florida (2009).
- ³⁵ H. Böttger and G. Kasner, *Phys. Stat. Sol. B* **158**, 143 (1990).
- ³⁶ M. Engel, S. Sonntag, H. Lipp, and H. R. Trebin, *Physical Review B* **75**, 144203 (2007).
- ³⁷ L. Li and X. Yang, *Physica B* **403**, 2888 (2008).
- ³⁸ R. K. Pattnaik and E. A. Whittaker, *Journal of Physics A* **25**, 577 (1992).
- ³⁹ R. Ilan, E. Liberty, S. E. Mandel, and R. Lifshitz, *Ferroelectrics* **305**, 15 (2004).
- ⁴⁰ G. Urban and J. Wolny, *Journal of Non-Crystalline Solids* **334–335**, 105 (2004).
- ⁴¹ G. P. P. Pun, V. Yamakov, and Y. Mishin, *Modelling and Simulation in Materials Science and Engineering* **23**, 065006 (2015).
- ⁴² S. M. Foiles, M. I. Baskes, and M. S. Daw, *Physical Review B* **33**, 7983 (1986).
- ⁴³ C. A. Becker, F. Tavazza, Z. T. Trautt, and R. A. Buarque de Macedo, *Curr. Opin. in Solid State and Mats. Science* **17**, 277 (2013).
- ⁴⁴ G. P. P. Pun and Y. Mishin, *Phil. Mag.* **89**, 3245 (2009).
- ⁴⁵ G. P. P. Pun and Y. Mishin, *Phys. Rev. B* **86**, 134116 (2012).
- ⁴⁶ J. Y. Park, D. F. Ogletree, M. Salmeron, R. A. Ribeiro, P. C. Canfield, C. J. Jenks, and P. A. Thiel, *Physical Review B* **74**, 024203 (2006).
- ⁴⁷ J. Y. Park, D. F. Ogletree, M. Salmeron, C. J. Jenks, P. A. Thiel, J. Brenner, and J. M. Dubois,

Journal of Materials Research **23**, 1488 (2008).

- ⁴⁸ J. Y. Park, D. F. Ogletree, M. Salmeron, R. A. Ribeiro, P. C. Canfield, C. J. Jenks, and P. A. Thiel, Physical Review B **71**, 144203 (2005).
- ⁴⁹ J. Hafner, M. Krajči, and M. Mihalkovič, Phys. Rev. Lett. **76**, 2738 (1996).
- ⁵⁰ M. A. Chernikov, H. R. Ott, A. Bianchi, A. Migliori, and T. W. Darling, Phys. Rev. Lett. **80**, 321 (1998).
- ⁵¹ F. Dugain, M. de Boissieu, K. Shibata, R. Currat, T. J. Sato, A. R. Kortan, J.-B. Suck, K. Hradil, F. Frey, and A. P. Tsai, Eur. Physical J. B **7**, 513 (1999).
- ⁵² C. Dong, L. Zhang, Q. Zhou, H. Zhang, J. Dubois, Q. Zhang, Y. Fu, F. He, and F. Ge, Bull. Mats. Sci. **22**, 465 (1999).
- ⁵³ S. Sinnott, Private communication.
- ⁵⁴ N. N. Gosvami, M. Feldmann, J. Peguiron, M. Moseler, A. Schirmeisen, and R. Bennewitz, Phys. Rev. Lett. **107**, 144303 (2011).